Research Square

Preprints are preliminary reports that have not undergone peer review.
They should not be considered conclusive, used to inform clinical practice,
or referenced by the media as validated information.

Flexible roll bending process and improved forming characteristics of integral panel with an elastomer-covered roller system

Min Zhang

zm@xpu.edu.cn

Xi'an Polytechnic University

Chihang Zhang
Wenbin Tang
Guang Lu
Pengle Cao

Research Article

Keywords: Flexible roll bending, Integral panel, Polyurethane elastomer, Generatrix straightness, Curvature radius

Posted Date: February 26th, 2026

DOI: https://doi.org/10.21203/rs.3.rs-8738838/v1

License: This work is licensed under a Creative Commons Attribution 4.0 International License.
Read Full License

Flexible roll bending process and improved forming characteristics of integral panel with an elastomer-covered roller system

Min Zhang*, Chihang Zhang, Wenbin Tang, Guang Lu, Pengle Cao

School of Mechanical and Electrical Engineering, Xi'an Polytechnic University, Xi'an, China

*Corresponding author: zm@xpu.edu.cn

Abstract

The manufacturing of next-generation aerospace components demands integral aluminum alloy panel that combine large dimensions, light weight, and high precision. Conventional rigid roll bending, however, often results in surface concavity and rib buckling during the forming of such thin-walled structures. Here, a flexible roll bending process using an elastomer-covered roller system is proposed to mitigate these issues. A finite element model of the forming process for high-strength aluminum alloy integral panel is established and experimentally validated. The influence of elastic layer hardness and press amount on stress distribution, curvature radius, and generatrix linearity are systematically investigated. The results reveal that, compared to rigid roll bending, the flexible approach achieves a markedly more uniform stress distribution across stiffened ribs, with a 34.3% reduction in peak stress. At an optimal press amount of 17.5 mm and an elastic layer hardness of 95A, generatrix straightness coefficient is improved by 51.6%. This work establishes a robust framework for advancing roll forming techniques in the fabrication of high-performance integral aerospace structures, offering both a viable manufacturing strategy and theoretical support.

Keywords: Flexible roll bending, Integral panel, Polyurethane elastomer**,** Generatrix straightness**,** Curvature radius

1 Introduction

Aluminum alloy integral panels with cross-net stiffened ribs can achieve lightweight while ensure high strength and load-bearing performance. They are widely used in the fields of aerospace, marine, automobile and engineering structure owing to their advantages such as high strength, low weight, high efficiency, and strong reliability [1-4]. However, the integration of high-density, spatially interlaced ribs into large-scale integral panels introduces profound geometric and mechanical constraints, including complex shapes, significant variations in cross-sectional dimensions, uneven thickness, and high requirements for surface accuracy (forming error less than 0.5mm), which bring new problems and challenges to their forming and manufacturing technology [5,6].

The roll bending forming process is widely used for manufacturing panel-type components due to its simple structure, excellent processing continuity, cost-effectiveness and energy-saving [7,8]. Currently, roll bending forming processes for integral panels include traditional roll bending and filling roll bending. At present, there are two kinds of traditional roll bending forming process, one is the rigid roll direct roll bending forming process [9,10], based on the deformation principle of three-point bending, the upper roll is similar to the upper head of three-point bending. In this process, the main defects such as concave skin surface and buckling instability of steel bar often occur. Due to the direct contact between the rigid roller and the siding during rolling and bending, especially in the surface area of the rib, which causes stress concentration, while the central area of the skin away from the rib is subjected to less stress, resulting in serious damage to the mechanical properties and geometry of the siding. The other is the rigid roller packing assisted rolling bending [11-14]. This method solves the instability deformation defects of the mesh bars and thin walls in the rolling bending process of the high-reinforcement thin-wall sheet through the auxiliary rolling bending of the mesh bars and rubber materials after milling, realizes the bending formation of the ultra-large mesh sheet, improves the straightness accuracy of the bus bar, and solves the difficult problem of manual calibration of the ultra-large wall sheet. Li HW. et al. [12] investigated the polypropylene filler-assisted roll forming process for 2A12 aluminum alloy panels and revealed the mechanism by which the filler improves the forming accuracy of stiffeners and skin by reducing the position deviation of the neutral layer. Zhang SH et al. [14] proposed a filler-assisted roll forming technique for grid-stiffened panels. Experimental studies were conducted using rubber and plastic fillers, which verified that the proposed method effectively reduces buckling instability and skin indentation

defects. In addition, the theory of flexible roll forming has been continuously developed both domestically and internationally. However, the preparation of the filler required by this process needs to be customized according to the specific type of wall slab bar, and the filler needs to be filled and cleaned before and after the rolling and bending process, which consumes a lot of manpower and is not conducive to mass production. These factors limit its wide application in practical production.

Flexible roll bending, as an advanced continuous bending forming technology, is characterized by high forming accuracy, fast speed, and excellent surface quality. It can be divided into single axis flexible rolling forming [15,16], double axis flexible rolling forming [17-21] and curved surface flexible rolling forming [22-27]. The single-axis flexible rolling bending process realizes the consistency of workpiece feed and bending. double axis flexible rolling forming can realize single curvature machining of large thin plate structure with uniform thickness, which solves the problem of "straight edge effect" of traditional process quality, omits the step of removing straight edge of traditional process, and is mainly used in bending process and rolling process before opening sleeve welding. Flexible rolling and bending of curved surface can realize multi-curvature machining. Yang KY et al. [20] developed a finite element model of double-roll flexible roll forming based on the ABAQUS platform to simulate the forming process of 3J21 spring steel strips. Zhang T. et al. [21] conducted biaxial flexible roll forming experiments on circular and elliptical parts and obtained the relationship between the forming curvature radius and the indentation depth. Chen P. et al. [22] investigated the surface forming mechanism in four-roll flexible rolling forming processes. The issues of low efficiency and significant residual stresses were addressed. Wei ZD et al. [23] proposed a multi-radius local bend forming methods for flower pattern and flexible roll profile, and the flexible rolls spatial positioning for thin-walled round pipes. The results indicate that the flexible forming of thin-walled round pipes with multiple specifications can be successfully achieved. Salem J. et al. [24] developed an analytical prediction model to predict the roll forming force, residual stress, and bending radius during the forming of cylindrical and conical parts. Fu Z. et al. [25] proposed an analytical model for the three-roll forming process and established a finite element model (FEM) using ABAQUS, deriving a reasonably accurate relationship between the downward displacement of the inner roll and the required springback radius (unloading curvature radius), and optimized the structural dimensions and process parameters. Li Shi et al. [26] developed an analytical model considering springback to correlate process parameters with the coiling radius and confirmed its effectiveness in improving forming accuracy. At present, most domestic and international studies on roll forming processes focus on plates with uniform thickness, while research on roll forming of grid-stiffened integral panels remains limited. Fan ST et al. [27] built a finite element simulation model for roll forming and validated its feasibility for simulating the coiling process of wide plates through experiments.

In summary, current flexible roll-bending processes are primarily applied to the forming of metal plates and strips. However, the flexible roll bending of aluminum alloy integral panels with complex structures remains insufficiently explored. To address existing challenges—such as surface concavity of the skin, buckling and instability of ribs, and poor consistency in the curvature radius during the flexible roll-bending of integral panels—this study proposes a novel flexible roll-bending method for aluminum alloy integral panels, wherein an elastic layer is covered on the outer surface of the rigid roller. A finite element model of the flexible roll-bending process is developed based on the Mooney–Rivlin hyperelastic-plastic material model. The effects of the elastic layer's hardness and the press amount on the curvature radius, stress distribution, and straightness of the generatrix of the entire panel are systematically investigated. The proposed method provides a viable roll bending forming strategy and theoretical support for the fabrication of high-performance integral aerospace structures.

2 Methodology

2.1 The principle of flexible roll-bending forming process

The principle of flexible roll bending forming is illustrated in Fig.1. The upper roller is a flexible roller, which is composed of a rigid transmission shaft and a polyurethane rubber coated on it. The two lower rollers are rigid rollers arranged horizontally symmetrically. The flexible roll bending process has two stages. In the first stage, after the downward pressure P is applied to the rigid drive shaft of the upper roller driven by the motor, the flexible roller produces a downward pressure D along the vertical direction under the pressure, so that the polyurethane rubber layer of the flexible roller is elastically deformed. With the increase of the pressing amount, the contact area between the flexible roller and the whole panel increases gradually. The elastic layer of the flexible roller falls into the groove of the wall plate to provide support for the ribs and skin.

Thus, the problem of small contact area and serious stress concentration when the traditional rigid shaft is directly rolled is effectively improved. In the second stage, when the flexible roller reaches the set downward position, the elastic layer of the flexible roller is in close contact with the outer surface of the skin and the outer surface of the ribs of the integral panel. Subsequently, when the flexible roller actively rotates, the friction between the elastic layer and the outer surface of the integral panel ribs, the friction between the rigid roller and the outer surface of the integral panel skin, drives the integral panel to feed forward automatically. This process achieves continuous bending forming, and promotes the overall panel to reach the desired bending shape through continuous local plastic deformation. Therefore, the pressing amount of the upper roller and the hardness of the elastic layer are the key factors affecting the forming radius and quality of the plate.

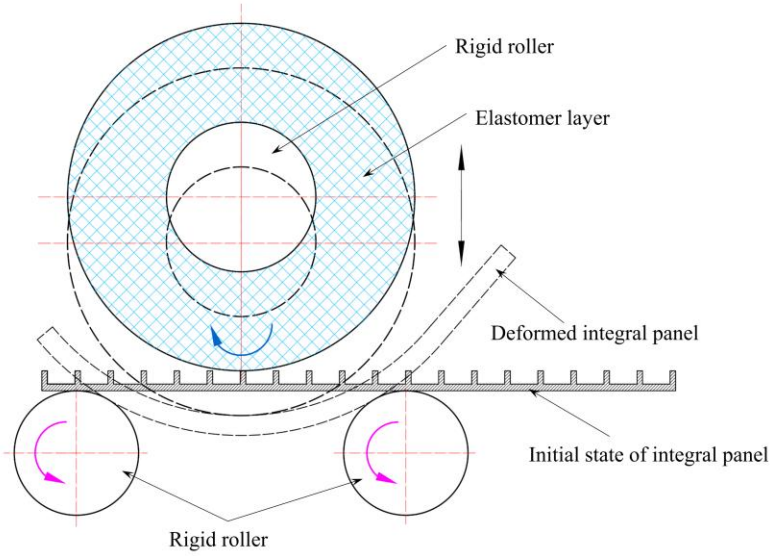


Fig. 1 The principle of flexible roll bending forming

2.2 Generatrix straightness

Generatrix straightness (ΔH) is defined as the offset between the theoretical contour (S_r) of the bus line on the outer surface of the integral panel skin and the actual contour (S_t). This deviation is consistently measured along the normal direction to the panel's curvature, as illustrated in Fig 2. To ensure measurement accuracy, the measurement plane of the bus bar gauge must remain aligned with the normal direction of the panel's curvature.

$$\Delta H = | S_r - S_t | = \sqrt{(X_{\max} - X_{\min})^2 + (Y_{\max} - Y_{\min})^2} \tag{1}$$

In the equation, ΔH represents the deviation of the bus line straightness, S_r denotes the actual contour, and S_t represents the theoretical contour. The actual contour Sr consists of N discrete nodes, with S_{ri} (X,Y) denoting the coordinates of the i-th node.

The generatrix straightness coefficient (K_m) is closely related to the generatrix deviation and the width of the integral panel. A smaller coefficient indicates a lower deviation, resulting in less pronounced surface depression defects on the panel skin and thereby reflecting higher forming precision of the integral panel.

$$K_m = \frac{\Delta H}{B} \tag{2}$$

where K_m denotes the generatrix straightness coefficient, and B represents the width of the integral panel.

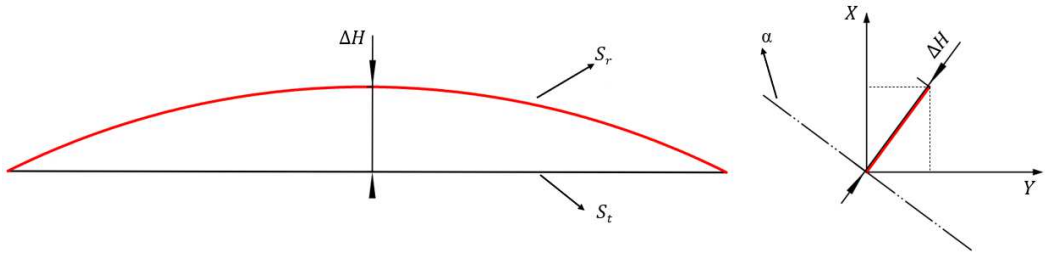


Fig. 2 Characterization of generatrix straightness

As shown in Fig.3, to evaluate the shape quality of the wall panel during the roll-bending process, six equally spaced sampling positions are defined along the longitudinal direction of the bent panel. At each sampling section, nodal displacement data are extracted from the finite element simulation along the generatrix direction of the panel. Based on these data, the generatrix straightness deviation and the corresponding straightness coefficient are calculated to quantitatively assess the shape accuracy of the panel skin.

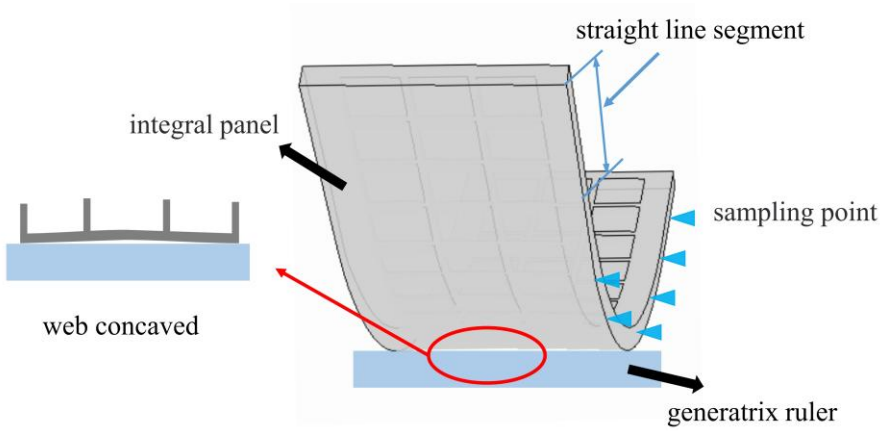


Fig. 3 Illustration of generatrix straightness of the integral panel

2.3 Curvature radius

During the flexible three-roll bending process, due to its foundation in the three-point bending principle, a localized straight-edge effect tends to occur at the front end of the wall panel during the initial stage of roller indentation. Therefore, to accurately characterize the post-forming bending radius, it is necessary to select the region of the wall panel that remains in a state of uniform bending as the analysis area.

To determine the formed bending radius, the nodal coordinates along the geometric neutral layer of the panel are extracted to form the dataset $R\{x_i, y_i\}$, upon which an arc fitting is conducted using the least squares method. The general equation of a circle in Cartesian coordinates is:

$$(x-x_c)^2+(y-y_c)^2=r^2 \tag{3}$$

Where (x_c, y_c) is the center of the circle, r is the radius of the circle.

The objective function for least squares circle fitting aims to minimize the sum of squared differences between the actual distances of data points to the estimated circle center and the estimated radius. the least squares objective function is:

$$\min_{x_c,y_c,R}\sum_{i=1}^{n}\left[((x_i-x_c)^2+(y_i-y_c)^2-r^2)^2\right] \tag{4}$$

Combining Equations (3) and (4), the fitted arc radius r is derived, which accurately characterizes the bending radius of the formed integral panel.

3 Simulation and validation

3.1 Profile and roller dimensions

According to the actual overall panel structure, the geometric structure and dimensional parameters of the integral panel specimen were designed. The grid type of the wall panel was a square grid. The height of the rib is 6 mm and the width is 3 mm. The internal fillets of the grid ribs of the integral panel will be generated during the milling process. In the finite element simulation process, in order to improve the calculation efficiency of the finite element model, the internal fillets of the integral panel grid are simplified to right angles, as shown in Fig. 4a,b. The size of the rigid roller and elastomer are shown in Fig. 4c, the rigid roller diameter is 60mm, the thickness of the elastomer layer is 50 mm, and the length of the roller is 110 mm.

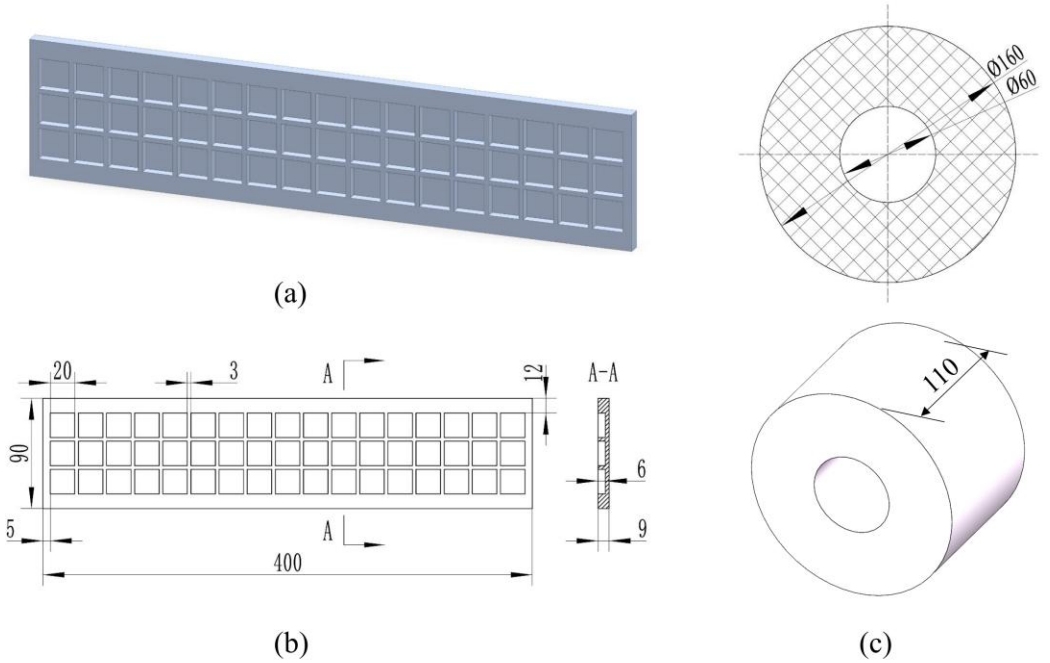


Fig. 4 The geometrical parameters of integral panel and roller (**a**) The 3D model of Integral panel specimen (**b**) The dimension of Integral panel specimen (**c**)Contact roller

3.2 Establishment of FE model for flexible roll bending

Geometric model

Finite element simulation has been extensively applied in the elastic–plastic analysis of materials, offering an effective means to address complex nonlinear problems and to visually reproduce the forming processes and deformation behaviors. The Abaqus software was employed to simulate the flexible roll bending process. To enhance the computational efficiency of the finite element analysis while ensuring result accuracy, reasonable model simplifications are implemented. Firstly, the driving effect of the transmission shaft on the elastic layer is simulated by coupling the nodes on the inner surface of the polyurethane elastomer with the centroid points of the transmission shaft. This approach simplifies non-essential components, reduces the number of contact pairs, and streamlines the contact interactions within the model. Secondly, given that the lower roller exhibits significantly higher stiffness compared to the integral panel, it is modeled as a rigid body component to effectively decrease the computational cost. Finally, during the roll forming process, rolling friction primarily occurs between the wall panel and each roller, accompanied by minor tangential sliding friction. By constraining the panel's movement in the width direction, sliding friction in this direction is neglected, which further simplifies the model and improves computational efficiency.

The finite element model of the roll bending forming process consists of one flexible roller, two rigid rollers, and the integral panel. The center distance between the two lower rollers is A=150 mm, and the initial gap between the upper roller and the top surface of the wall panel is H= 3 mm, as illustrated in Fig. 5.

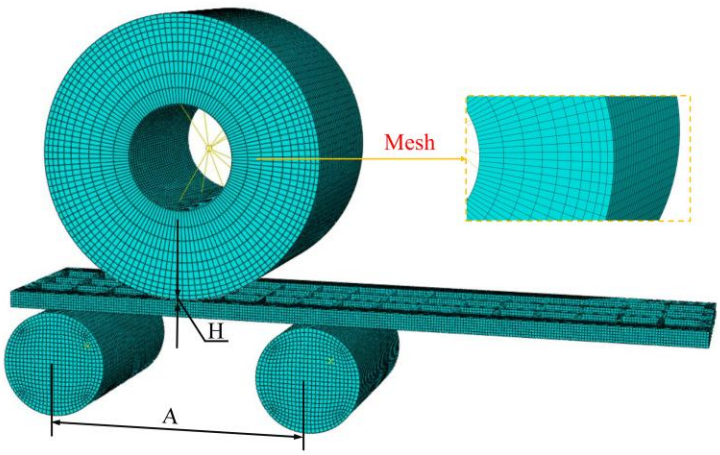


Fig. 5 FE model of flexible roll bending forming

The flexible roll bending process involves large deformation of elastic materials. Therefore, an explicit dynamic solver was selected for the analysis. The longitudinal downward pressing was simulated over a duration of 1 s, while the active rotation of the flexible roller was simulated over 2 s. The two lower rollers were modeled as rigid bodies, whereas the flexible roller and the integral panel were modeled as deformable bodies. All components have regular geometric shapes, thus hexahedral elements were used for meshing to ensure high computational accuracy and efficiency. During the roll bending process, significant mesh distortion occurred in the outer elastic layer of the flexible roller. To improve simulation accuracy, mesh refinement was applied to this outer elastic layer. The integral panel mesh size was approximately 1 mm × 1 mm, resulting in 59,844 elements. The mesh size of the flexible roller's elastic layer was approximately 2 mm × 2 mm, resulting in 35,280 elements.

Material properties

The high-strength aluminum alloy integral panels are made of 7050-T7451 aluminum alloy, which is widely used in aviation, aerospace, automotive and other fields. The mechanical property parameters of the material are shown in Table 1.

Table 1 Properties of AL 7050-T7451

Properties	Density ($g \cdot cm^{-3}$)	tensile strength (MPa)	yield strength (MPa)	Young modulus (MPa)	Poisson's ratio
Magnitude	2.83	502	442	66000	0.33

Polyurethane rubber was adopted as the elastic layer material in this study. Polyurethane rubber is a typical superelastomer, featuring significant nonlinear mechanical response, large deformation capacity and approximately incompressible properties [28,29]. In the finite element analysis software ABAQUS, the hyperelastic material is usually described by the strain energy density function U. Commonly used models include Mooney-Rivlin model and Neo-Hook model. The Mooney-Rivlin model effectively describes the mechanical behavior of polyurethane rubber under large deformation and nonlinear conditions, and is suitable for analyzing its complex deformation response during roll bending. In this paper, the Mooney-Rivlin model is used to characterize the superelastic behavior of polyurethane rubber. The expression of the strain energy density function of this model is as follows:

$$U = C_{10}\left(I_1 - 3\right) + C_{01}\left(I_2 - 3\right) + \frac{(J-1)^2}{D_1} \tag{5}$$

Among them, U is the strain potential energy, I_1 is the invariant of the first strain bias, I_2 is the invariant of the second strain bias, J is the volume ratio, C_{10} and C_{01} are Rivlin coefficients, and D_1 is the incompressible parameter of the material. For the rubber material constants C_{10} and C_{01}, methods such as uniaxial stretching, biaxial stretching, planar shearing and simple shearing are usually adopted. Among them, the tensile stress σ, tensile ratio λ of the rubber material and the material constants C_{10} and C_{01} can be expressed by the following formula:

$$\frac{\sigma}{2(\lambda - 1/\lambda^2)} = C_{10} + C_{01}/\lambda \tag{6}$$

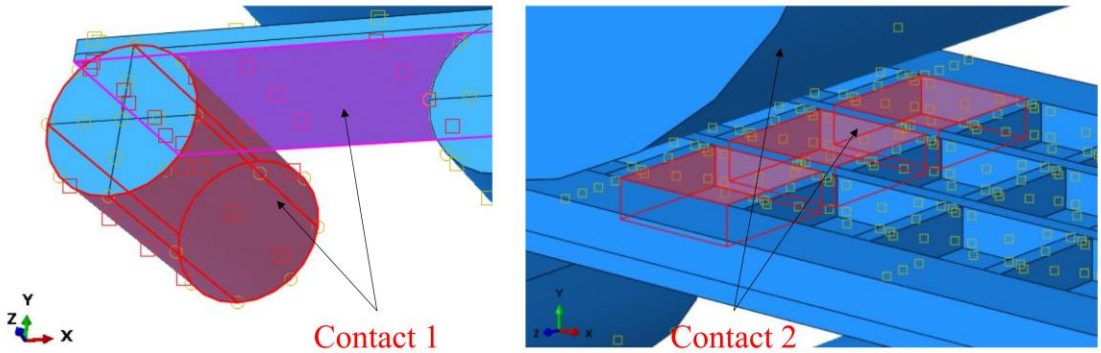
Based on the research and experiments of relevant scholars, the constants of polyurethane rubber materials in the Mooney-Rivlin model are shown in Table 2.

Table 2 Mooney-Rivlin Model Polyurethane Rubber Material Constant

Hardness	C_{10}	C_{01}
95A	3.58	0.48
85A	1.41	0.4

Contact definition and constraint

The flexible roll bending forming process of the integral panel involves complex multi-body contact interactions, which can be categorized into two primary contact pairs. The first contact pair occurs between the outer surfaces of the two lower rollers and the bottom surface of the integral panel (i.e., the outer surface of the skin). The second contact pair is established between the upper surface of the integral panel (i.e., the outer surface of the stiffening ribs) and the outer surface of the flexible roller (i.e., the elastic layer). Among these, the second contact interaction is more intricate due to the presence of groove structures in the rib region. When defining the contact surface on the upper side of the integral panel, the geometrical characteristics of these grooves must be accurately represented, as shown in Fig.6.



(a) (b)

Fig. 6 Contact Condition (**a)** Rigid roll and panel (**b)** Flexible roll and panel

All contact interactions in the finite element model are defined using the penalty method with finite sliding formulation. A friction coefficient of 0.25 is assigned between the integral panel and the rigid rollers, with the rigid rollers designated as the master surfaces. For the contact between the integral panel and the flexible roller, a higher friction coefficient of 0.45 is specified, and the flexible roller is defined as the master surface. In the master–slave surface assignment, selecting the component with lower deformation and a relatively finer mesh as the master surface helps mitigate mesh distortion during the contact computation, thereby enhancing the numerical stability and accuracy of the simulation.

Process Parameter and analogue simulation

By comparing different processes and two process parameters of hardness and press amount, the influence of flexible roll bending process on the bending forming law of integral panel is studied. The process parameter combination is shown in Table 1.

By comparing the two processes and the two process parameters of polyurethane hardness and pressure reduction, the influence of the flexible roll bending forming process on the bending deformation behavior of the overall wall panel was studied. The specific process parameters are as follows: The hardness of polyurethane is 85A and 95A respectively, and the reduction amounts are 17.5mm,20mm, and 22.5mm. The combination of process parameters is shown in Table 1.

Table 3 Process Parameter Combinations

No.	Bending type	Polyurethane hardness (Shore Hardness A)	press amount (mm)
P1	flexible roll bending	95	17.5
P2			20
P3			22.5
P4		85	17.5
P5			20
P6			22.5

3.3Validation of the numerical model

The integral panel is milled as shown in Fig.7a. The flexible roll bending forming process can be equivalently regarded as three-point bending at multiple consecutive positions. Based on this, three-point bending tests of the integral panels with the elastic coating layer were carried out on the E45.305 electronic universal testing machine, and the loading speed of the flexible head was 1 mm/min, as shown in Fig.7b. The experiment employed a polyurethane rubber elastic layer with a hardness of 95A, with compression depths set at 17.5 mm and 22.5 mm respectively. Each operating condition was tested three times, with the average value recorded. Force-displacement relationship curves were obtained experimentally, and the bending angles of specimens after unloading were measured using a YHD OMQ190 optical coordinate measuring machine, as shown in Fig.14c. Results indicate that the maximum error in force-displacement response predicted by the finite element model did not exceed 14.31%, while the bending angle prediction error remained below 14.19%. This validates that the established finite element model's accuracy meets engineering application requirements and can be employed for research into the flexible roll-forming process of integral panels, as shown in Fig.7d.

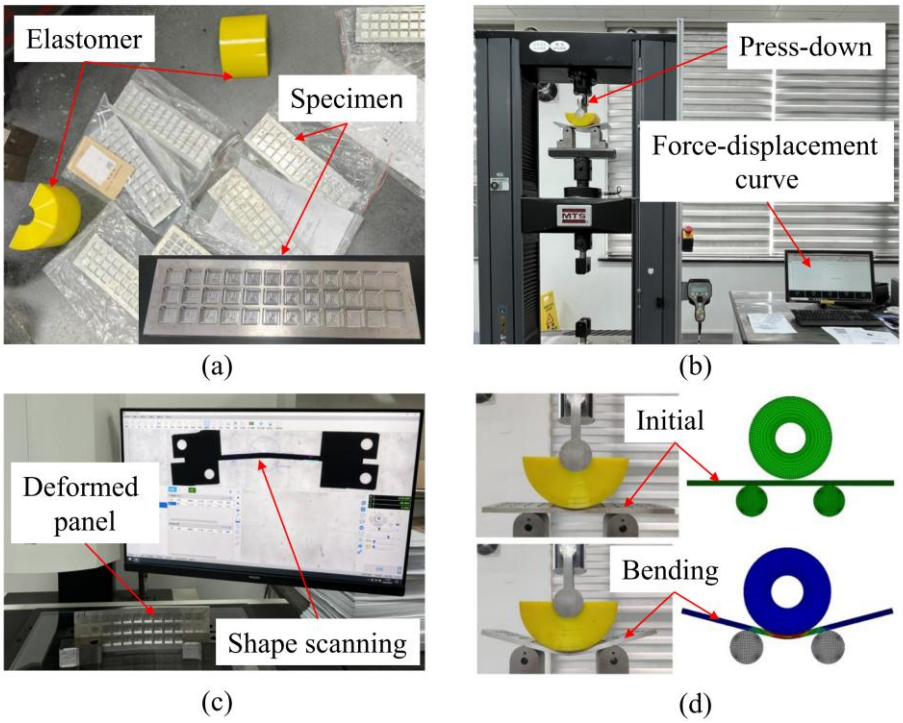


Fig. 7 Experimental verification

4 Results and discussion

4.1 Comparison of stress uniformity

By conducting rigid and flexible roll bending simulations on the integral panels respectively, the system obtained the stress distribution laws under different process paths, and the results are shown in Fig.8.

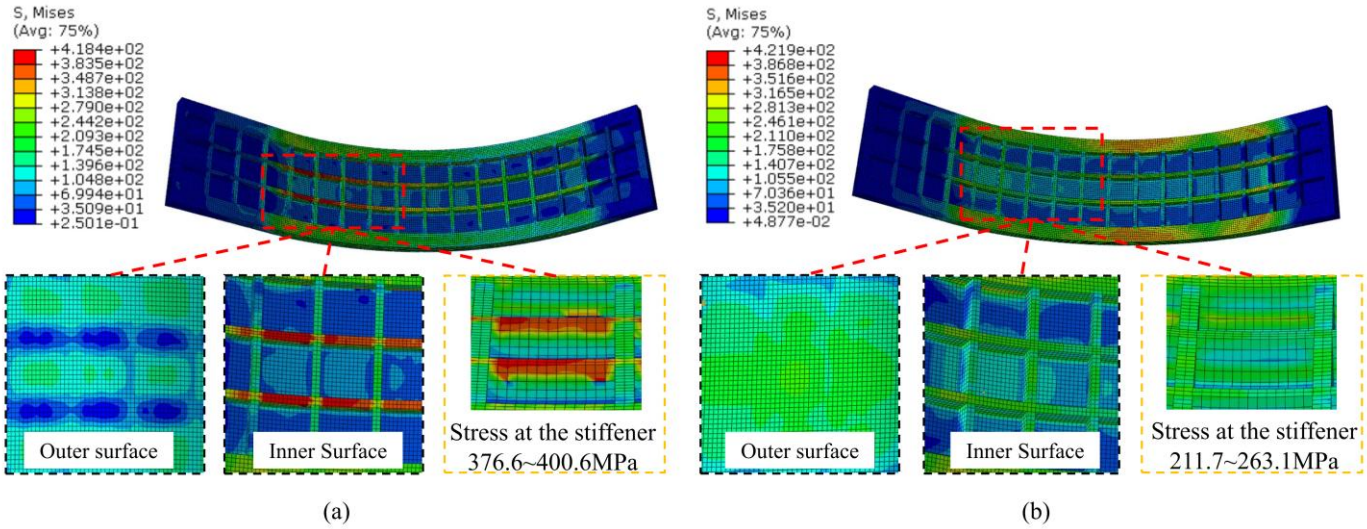


Fig. 8 Comparison of **(a)** rigid roll bending and **(b)** flexible roll bending

Under the rigid roll bending process, the equivalent stress in the rib regions of the wall panel reaches its peak value of 400.6 MPa during the initial downward pressing stage. In contrast, the equivalent stress remains relatively low throughout the subsequent continuous bending phase. This is due to the rigid three-roll bending forming process. During the downward pressing stage, the contact interface between the rigid roller and the integral panel corresponds to the outer surface of the stiffening rib, where the contact area is relatively limited.

In comparison, the flexible roll bending process yields a more uniform stress distribution across both the downward pressing and continuous bending stages, with the equivalent stress reaching a maximum of 263.1 MPa. It can be seen that the flexible roll bending forming process effectively improves the contact condition with a relatively small contact area during the roll bending and pressing stage, thereby making the pressure on the ribs more uniform and effectively avoiding the instability and deformation of the ribs.

To further investigate the stress variation characteristics in the rib region, a comparative analysis was conducted based on finite element simulation results of the local ribs. The study focused on the stress distribution of the tensile surface (i.e., the outer surface of the skin) and the compressive surface (i.e., the outer surface of the ribs) of the integral panel.

As Fig.8a shows, during the rigid roll bending process, on the compressed surface, the residual stress at this position is mainly concentrated on the transverse bars, and the stress at the center of the skin grid is relatively large. The stress distribution is uneven in both the transverse and longitudinal directions. There are obvious stress faults from the middle and lower parts to the root of the transverse bars. The stress at the transverse center is relatively small, while the stress on both sides is relatively large. On the tensile surface (the outer surface of the skin), the stress distribution presents a ring-shaped structure with the center of the skin as the core, and the stress gradually increases as the distance from the center position decreases, indicating that this area is subjected to a strong tensile load. Meanwhile, in the rolling and bending direction, the equivalent stress in the connection area between the skin and the transverse bars is significantly lower than that in the surrounding area.

As Fig.8b shows, the stress distribution characteristics of the integral panel under the flexible roll bending process. On the compressed surface (the outer surface of the ribs), the stress distribution in the transverse rib area is more uniform, and the stress in the area originally in the low-stress zone inside the skin grid has increased, effectively alleviating the stress concentration phenomenon. No obvious stress faults appeared in the middle and lower parts to the root area of the transverse

bars, and the stress distribution in the longitudinal direction also tended to be consistent, indicating that flexible roll bending is helpful to improve the force continuity of the bar structure.

On the stretched surface (the outer surface of the skin), the equivalent stress values at the edge area of the skin and the junction of the skin and the transverse ribs are basically the same. The stress distribution along the width direction of the wall panel and the rolling direction is relatively uniform, further indicating that flexible rolling can effectively improve the stress balance of the wall panel after forming.

Overall, the flexible roll bending process has significantly improved the residual stress distribution characteristics of the integral panels. Compared with the traditional rigid roll bending process, the maximum equivalent stress at the lower rib in the flexible roll bending has decreased from 400.6 MPa to 263.1 MPa, with a reduction of 34.3%. This significant difference indicates that the elastic layer material of the flexible roller expands the force-bearing contact area of the ribs during the deformation process, thereby achieving a more uniform load distribution in the width direction and the rolling direction of the wall panel, and significantly improving the stress uniformity of the overall wall panel.

4.2 Influence of forming radius

To explore the influence of roll bending process parameters on the forming quality of the integral panel, the influence laws of the roller downward pressure and the hardness of the elastic layer material of the flexible roller on the curvature radius and the straightness of the generatrix of the formed wall panel were studied. The simulation results are shown in Fig. 9.

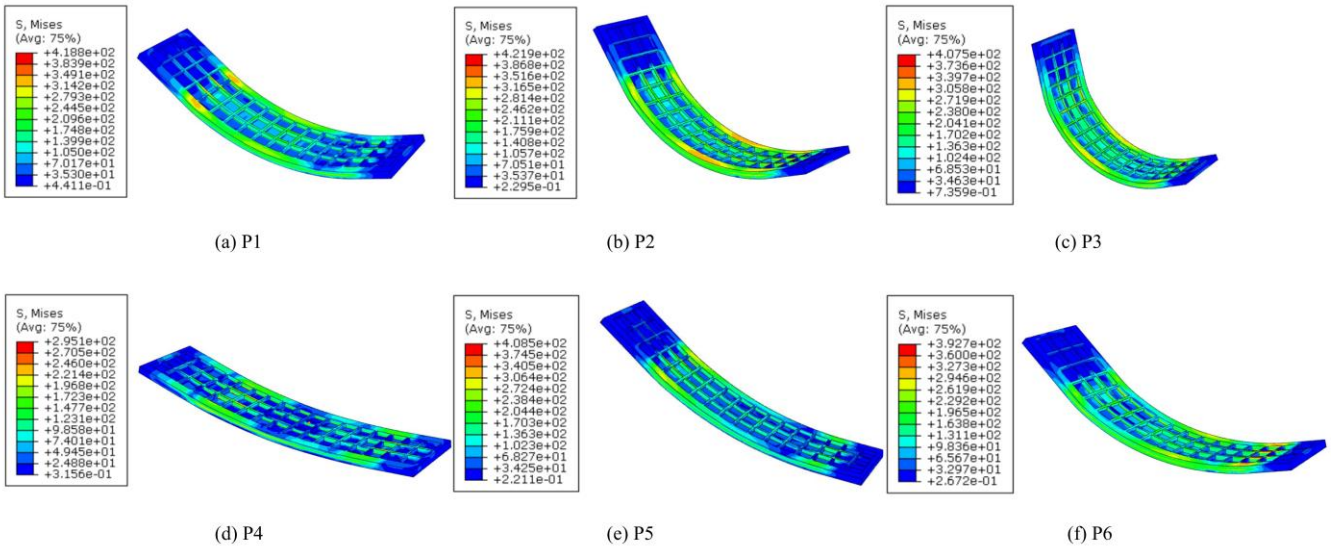


Fig. 9 Simulation results of roll bending with different process parameters

Based on the neutral layer theory of plate parts, the bending characteristics of the whole wall panel are analyzed and the coordinates of the neutral layer are extracted, as shown in the Fig.10.

It can be seen that the six curved contours all have small straight sections at the ends. This is because the flexible rolling bending is based on the three-point bending principle, so a straight edge phenomenon will occur at the front end of the panel after forming. It can be seen from the bending profile that the radius of curvature at the initial position of roll bending is smaller than that at the continuous roll bending stage. This is because at the initial position of roll bending, the rolling speed is relatively small, the contact time between the roller and the wall plate is longer, the accumulation of stress during the roll bending process increases, and the time for plastic deformation to occur is longer. During the continuous roll bending stage, there is a certain uniform speed, so the forming radius increases.

To avoid the curvature deviation caused by the straight edge effect, the curvature profile of the continuous roll-bending section is taken in the study of the influence of the curvature radius.

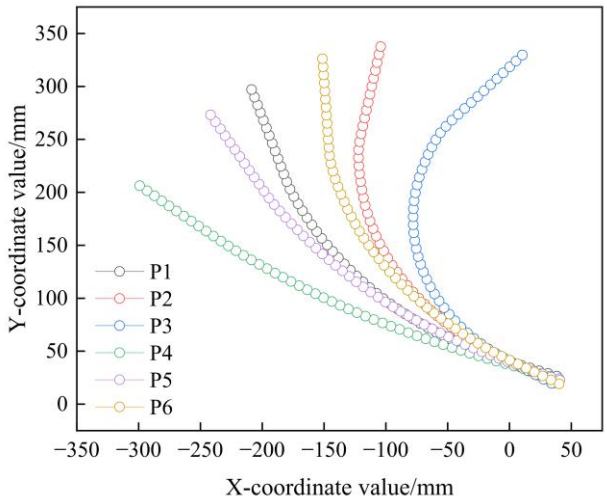


Fig. 10 Bending profile results with different hardness and different pressure

In order to analyze the influence of the hardness of different elastic layers on the curvature radius of the overall wall panel, the coordinate values of a row of nodes along the bending direction after roll bending were taken from the above results, and the corresponding forming diameter was obtained by fitting the coordinates through the least square method. Fig.11 shows the relationship between the hardness of the elastic layer and the curvature radius of the wall panel. It can be seen from the figure that the curvature radius gradually decrease as the downward pressure increases. This is because as the downward pressure increases, the overall wall panel is subjected to greater deformation force, and the plastic deformation area during the forming process increases, resulting in a decrease in the forming curvature radius.

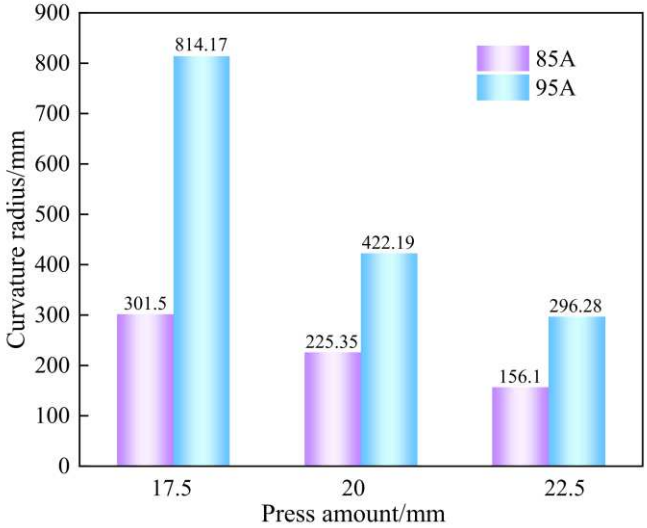


Fig. 11 The relationship between forming radius and pressure of polyurethane wheel with different hardness.

4.3 Influence of Generatrix straightness

In the process of continuous roll bending, the straightness of the busbar changes with the position as shown in Fig.12a. It can be observed that with the advancement of the roll bending process, the generatrix straightness shows a decreasing trend. This is mainly due to the uneven distribution of the force of the roller on the panel in the time dimension, resulting in differences in the degree of plastic deformation in the local area of the panel. The maximum deviation of bus straightness at different positions is up to 20 %. The maximum deviation values of the 6 groups of data appear at the initial downward pressure position. Due to the low speed of the roller at this position, the wall plate undergoes longer stress accumulation in

this area, resulting in more obvious plastic deformation, which in turn causes a large deviation in the straightness of the busbar.

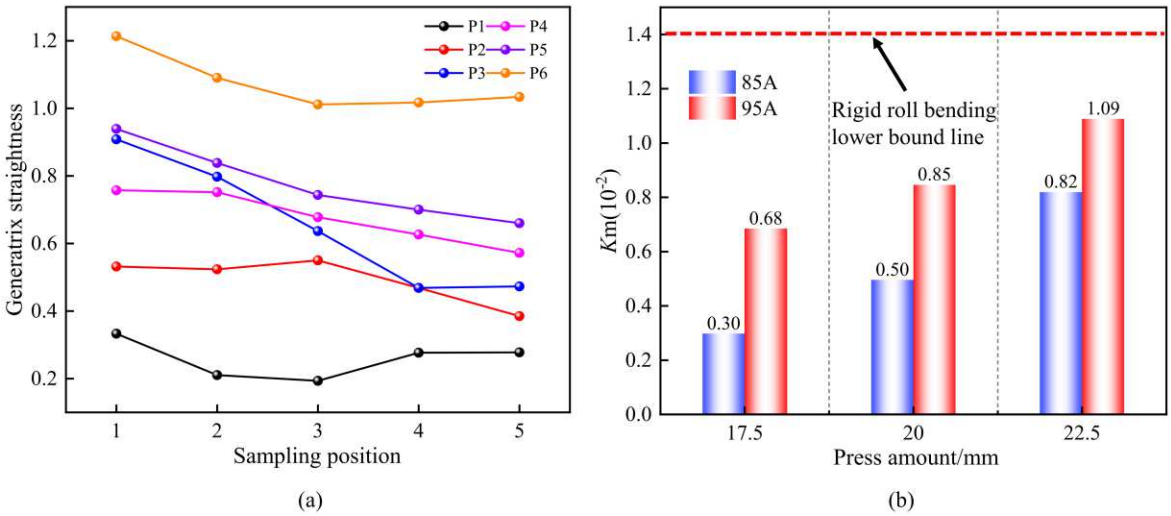


Fig.12 Bending profile results with different hardness and different pressure (**a)** The straightness of the generatrix at each sampling position (**b)** The straightness coefficient of busbars under different process parameters

Taking the maximum value of busbar straightness as the characterization index of busbar straightness of the whole panel, the evaluation standard of busbar straightness coefficient *K*m is established, as shown in Fig.12b. From the diagram, it can be seen that the straightness coefficient *K*m of the whole panel bus bar obtained by the six groups of flexible roll bending tests is lower than the minimum value of the bus bar straightness coefficient under the rigid roll bending process. When the pressing amount is 17.5mm and the hardness is 95A, the bus straightness coefficient *K*m is reduced by 51.6 %. This shows that the flexible roll bending process has a significant advantage in forming accuracy. In addition, under different process parameters, the bus straightness coefficient has a certain rule. Under the condition of the same elastic layer hardness, the bus straightness coefficient *K*m increases with the increase of the pressing amount. This is because a larger amount of press will cause a larger normal load, which will aggravate the plastic deformation of the local area of the panel and easily lead to concave defects in the panel. Therefore, the geometric deviation along the generatrix direction increases and the forming accuracy decreases. Under the same pressing amount, when the hardness of the elastic layer is low, the bus straightness coefficient is significantly smaller than the corresponding value under higher hardness conditions. This is because the low-hardness elastic layer has greater deformation capacity and greater compression deformation after compression, thereby reducing the actual effective pressing amount, resulting in a reduction in the bus straightness coefficient.

5 Conclusion

1) A flexible roll-bending process using an elastomer-covered roller system for the fabrication of integral panel is proposed and experimentally validated. This method provides a more uniform contact pressure during the forming process. This approach ensures more uniform contact pressure across the panel surface, significantly mitigating stress concentration and substantially reducing the risk of buckling defects commonly associated with conventional rigid roll forming.

2) Compared to rigid roll bending, the flexible approach achieves a markedly more uniform stress distribution across stiffened ribs, with a 34.3% reduction in peak stress. At an optimal press amount of 17.5 mm and an elastic layer hardness of 95A, generatrix straightness coefficient is improved by 51.6%.

3) The hardness of the elastic layer markedly influences the curvature radius, with greater hardness correlating with a smaller radius of curvature. The flexible process also yields superior generatrix straightness, consistently outperforming rigid roll bending. Optimal straightness is achieved at a press amount of 17.5 mm and an elastic layer hardness of 95A, resulting in a 51.6% improvement in straightness coefficient. These findings establish the flexible roll-bending method as a reliable and efficient strategy for producing high-integrity, lightweight aerospace panels.

Author contributions Min Zhang: conceptualization, methodology, validation, review and editing; Chihang Zhang: material preparation, analysis and visualization, writing-original draft. Guang Lu and Pengle Cao: software, analysis and visualization. Wenbin Tang: review and editing, supervision and guidance. All authors have read and agreed to the published version of the manuscript.

Funding This study was supported by the Natural Science Basic Research Project of Shaanxi Province, China [grant number 2022JQ-526, 2025JC-YBMS-381], the Educational Commission of Shaanxi Province, China [grant number 24JK0466], the Key Laboratory of Road Construction Technology and Equipment of MOE, Chang'an University [grant number 300102252508], the Doctoral Foundation Project of Xi'an Polytechnic University [grant number BS202121] and Innovation Fund for Postgraduates of Xi'an Polytechnic University [grant number chx2025009].

Availability of Data and Materials The data and materials are available from the authors upon reasonable request.

Declarations

Consent for publication Yes.

Competing interests The authors declare no competing interests.

References

[1] Lei YD, Zhan M, Fan XG (2022) A review on manufacturing technologies of thin-walled components with ribs. Journal of Northwestern Polytechnical University, 40(1):1–17
[2] Zhu ZW, Zhao YX, Ouyang YW, Yu ZQ, Chen XH (2025) Research on the two-step method in spin extrusion forming for thin- walled cylindrical rings with two-level ribs. Int J Adv Manuf Technol 141:6159–6178
[3] Alfawzan Y, Lv JX, Shi ZS, Lin JG (2025) An investigation of the curvature variation in rolling a stiffened panel. Int J Adv Manuf Technol 137:1565–1580
[4] Huang GY, Zhang YF, Wu T, Shi P, Wan MH (2025) Roll bending forming curvature radius prediction based on the CNN-TCN-TPA neural network model. International Journal of Material Forming 18:34
[5] Schneider F, Das J, Kirsch B, et al (2019) Sustainability in ultra precision and micro machining: A review. International Journal of Precision Engineering and Manufacturing-Green Technology,6(3):601-610
[6] Niemann S, Wagner HNR, Huhne C (2021) Anisogrid stiffened panel under axial compression: Manufacturing, numerical analysis and experimental testing. Thin-Walled Structures, 161:1-10.
[7] Badparva H, Naeini HM, Kasaei MM, AsI YD, Abbaszadeh B, Silva LFM (2023) Deformation length in fexible roll forming. Int J Adv Manuf Technol 125:1229-1238
[8] Jing YG, Jiang SS, Sun Q, Zhao Y, Song ZH, Meng XY, Li HZ (2023) Design and development of high precision four roll CNC roll bending machine and automatic control model. Scientific Reports 13:12954
[9] Qi RX, Sun SM, Yan SQ (2025) Numerical Investigation of Cold Roll-Forming Process for Three-Layer Metal Sheets and Al/ABS/Al Composites. Int J Steel Struct 25 338-349
[10] Jing YG, Kong DK, Sun Q, Zhao Y, Meng XY, Song ZH (2023) Analysis of the roll bending process of profile. Journal of the Brazilian Society of Mechanical Sciences and Engineering 45:373
[11] Xin YQ, Liu Q, Wang ZT, Li YJ, Liang HC (2025) Mechanical characteristics of the neutral layer and skin surface flatness in rigid-filled press-bending forming of magnesium alloy panels. Journal of Mechanical Science and Technology 39:6729-6738
[12] Li HW, Song HW, Zhang SH, et al (2023) Operating effect of filler on filling roll bending of integral panel. Transactions of Nonferrous Metals Society of China 33(8):2314-2327
[13] Nan SY, Zhang XL (2025) Optimization of the Elastic Modulus of the Filler in High-Rib Thin-Web Grid-Stiffened Panels with Bending Forming Process. Materials 18(16):3782
[14] Zhang SH, Xiao H, Liu JS (2009) Research on filling roll bending process of integral panel skin. Forging & Stamping Technology 34(02):54-56
[15] Wang GY, Li Q, Qian B (2012) Control System Development for Flexible Roll Forming Machine. Affective Computing and Intelligent Interaction 137:697-705
[16] Qian B, Li Q (2011) A Novel Control Procedure for Single Axis Roll Forming. Advanced Materials Research 181-182:177-182
[17] Hao T, Li XL, Du CF, et al (2022) Study on application of two-axis flexible roll bending technology for titanium alloy. Forging & Stamping Technology 47(2):83-87
[18] Duan YH, Wang JF, Lu SL, Cheng LH, Huang SW, Zhou K, Zhao YB, Li JC, Zhan XH (2025) Evolution mechanisms of residual stress in roll bending process for large-scale aerospace integral structures. Engineering Science and Technology, an International Journal 72:102214
[19] Simonetto E, Beigzadeh A, Ghiotti A, Bruschi S (2024) Evaluation of the effect of forming strategy in newly introduced flexible roll forming process. Manufacturing Letters 41:475-482
[20] Yang KY, Fang G, Zeng P, Lei LP, Zhang CF (2020) Three-dimensional finite element analysis of two-roller flexible bending process. Journal of Plasticity Engineering 27(8):31-38

[21] Zhang T, Sha H, Lu S, et al (2019) Study on flexible two-axis roll-bending process for component with non-circular section. Journal of Mechanical Science and Technology 33(9): 4421-4429
[22] Chen P, Lu SH (2024) Surface forming mechanism and numerical simulation study in four-roll flexible rolling forming. Heliyon 10(23):e40116
[23] Wei ZD, Cao JG, Zhu XD, Zhang ZY, Zhao RG (2025) Research on flexible roll forming process for manufacturing thin-walled round pipes with multi-specification. Journal of Manufacturing Processes 152:180-204
[24] Salem J, Champliaud H, Feng Z, et al (2016) Experimental analysis of an asymmetrical three-roll bending process. Int J Adv Manuf Technol 83(9-12): 1823-1833
[25] Fu Z, Tian X, Chen W, et al (2013) Analytical modeling and numerical simulation for three-roll bending forming of sheet metal. Int J Adv Manuf Technol 69(5-8): 1639-1647
[26] Li S, Qian YP, Zhang DQ, et al (2024) Rounding precision research on horizontal up-adjustable three-roll plate bending machine considering spring back. Journal of Plasticity Engineering 31(2):66-75
[27] Fan ST, Meng SF (2007) Simulation of the three-roll pyramid type plate bending machine multi bending process. Machinery Design & Manufacture (06):82-84
[28] Du XB, Zhao YQ, Lin F, Xiao Z (2017) Parameters determination of Mooney-Rivlin model for rubber material of mechanical elastic wheel Applied Mechanics and Materials 872:198–203
[29] Mehrara M, Nategh MJ (2011) Analysis of the elastic and plastic roll bending of sheet metal on a rubber pad. Proceedings of the Institution of Mechanical Engineers, Part B: Journal of Engineering Manufacture 226(4):722-732